



Issues and mitigation of interference, attenuation and direction of arrival in IEEE 802.15.4/ZigBee to wireless sensors and networks based smart building



H. Ghayvat*, S.C. Mukhopadhyay, X. Gui

School of Engineering and Advanced Technology, Massey University, New Zealand

ARTICLE INFO

Article history:

Received 17 July 2015

Received in revised form 11 January 2016

Accepted 28 January 2016

Available online 3 March 2016

Keywords:

Smart home

IEEE 802.15.4

Interference

Direction of arrival (DOA)

Attenuation

Radio signal

ABSTRACT

The performance metrics of IEEE 802.15.4 standard make it an only dominant option in short-range environmental monitoring and control applications. The heterogeneous sensor and actuator nodes based on the wireless technology are deployed into the smart building environment. Wireless technology deployed in building environment suffers from interference from different communication protocols operating in the same unlicensed ISM band, apart from the attenuation loss. A designer could not ignore these factors in the smart building because the adverse effect of these issues on system performance is considerable. Most of the researchers reported this but not with the aspects of the smart building. This research paper reports on the detailed experimental analysis and mitigation for different types of interference, the direction of arrival and attenuation losses associated with smart building condition. This research also tries to find the mitigation by direction of arrival of the radio signal. Our research aims to generate the customized methodology that will support and assist the smart building system designer to evaluate and measure the on-site performance so that these assessments will be precise, efficient and accurate. A realistic, smart home solution is applied to the building.

© 2016 Elsevier Ltd. All rights reserved.

1. Introduction

In the 21st century with the technological advancements, wireless sensor and networks (WSNs) has gained more and more attention for automation and monitoring by virtue of their easy installation and low costs. All over the place from mammoth structure building automation to the smart home, immense industrial applications in assembly units to health care services, space rocket program to tiny electronic gadgets by wireless sensors and networks, the WSN has produced the significant and important place in designing the modern world. The significant improvement by introducing the wireless technology

is that it reduces and simplifies the medium complexity and harness that sensing system gets in wired transmission, and offers facilitation for the installation of sensors, controllers, and actuators. The cost and installation efforts with an enlarged number of sensors in an urban environment are exponentially reducing by the wireless technology innovations [1,2].

Numerous types of wireless standards are documented; the implementation of any standard is a function of the application requirement. In the design of WSN various wireless communication technologies have been applied, such as WiFi, ZigBee, and Bluetooth. At home monitoring of the urban environment, short range, reliable data transmissions, and low power are the primary requirements. IEEE 802.15.4 ZigBee standard are widely accepted for a smart home solution. IEEE 802.15.4 offers lower layer

* Corresponding author.

E-mail address: ghayvat@gmail.com (H. Ghayvat).

(physical and data link) capabilities while ZigBee introduces upper layer functioning. This standard uses license-free industrial, scientific, medical (ISM) band, and ZigBee uses worldwide 2.4 GHz spectrum, which contains 16 channels numbered 11–26 and the data rate of 250 kbps [3]. Each channel with the bandwidth 2 MHz and channel separation of 5 MHz [4,5].

The IEEE 802.15.4 ZigBee standard enables the wireless technologies for heterogeneous sensors at home and building environment. The performance and facilities in wireless sensing are moving from research grade to the industrial stage as a smart building monitoring and automation. In the building environment various radio, communication devices are operating in the ISM band that causes the degradation in performance and reliability to desired radio signal between a sensor node and data collection points. There are three phenomena interference, attenuation, and multipath. The main issue with different wireless communications technologies in the same frequency band is that most of them are not appropriately planned to be compatible with each other. There are some concerns of channel overlapping as well. The co-existence behavior of Wi-Fi and ZigBee has been documented thoroughly in different research studies. Additionally physical layer concerns of Wi-Fi and ZigBee coexistence have previously considered in the IEEE 802.15.4 standard [6]. Even after this, the realistic building environment performance is totally different from the ideal IEEE standard consideration. There are other non-networking applications that emit the electromagnetic waves such as microwave in the ISM band that disturbs the wireless communication of personal area network (PAN). ZigBee protocol is based on Direct-Sequence Spread Spectrum (DSSS) technique. These spread spectrum technologies provide some degree of immunity from interferers [7,8].

The Physical lower layer behavior of Wi-Fi and ZigBee coexistence has been considered in different studies of WSNs design.

The existing research studies systematically consider the interference effects, but they are based on simulation approach. These studies conducted on several considerations for wireless communication environment, topology and interference sources. They used testbed assumptions such as worst case scenarios for experiments, which is totally different from realistic, practical building environment [9–12].

In the research [13] they found that the cross-technology estimation probability of Clear Channel Assessment (CCA) between ZigBee and Wi-Fi is critical. They identified that the Wi-Fi is insensitive towards ZigBee, but ZigBee is oversensitive to Wi-Fi. The CCA range for coexistence behavior was 25 m with free space path loss model. In the similar study by Tytgat et al. [14], they also presented that the CCA range of ZigBee can cut down the collisions with Wi-Fi, but the ZigBee CCA mechanism is a bit slow to avoid all Wi-Fi channel traffic. They recorded up to 85% ZigBee packet loss rate due to 802.11b contention. In the empirical data study by Sikora in [15], and extended in [16], an initial insight into the co-existence performance of IEEE 802.15.4 ZigBee is presented. It had recorded that with the channel offset of ~10 MHz the

packet error rate (PER) of IEEE 802.15.4 ZigBee reduces from 92% to 30%, under Wi-Fi interference. The setup had 2 m spacing between WPAN and Wi-Fi transmitter. In the similar research, Petrova et al. [17] briefly covered the co-existence with IEEE 802.11b/g. They performed experiments with the fixed spacing 3.5 m between Wi-Fi and WLAN and noted that for satisfactory performance of the IEEE 802.15.4 the offset frequency at least 7 MHz. For better co-channel rejection, the packets should be of small size. They recorded better system performance for the packets of 20 bytes as compared to the maximum packet size of 127 bytes. Wanqi et al. [18], in the research studies on impacts of 2.4 GHz ISM band interference on IEEE 802.15.4 WSN reliability in building environment noted that PER is ranging from 2% (no interference source) to 25% (interference source).

The other dominant interferer, Microwave oven, operates at around 2.45 GHz, and radiates a significant amount of electromagnetic signals. Although enclosed in a Faraday cage, it is still possible for some leakage to occur around the doors and opening. This gets worse over time as mechanical abuse or simple ‘wear and tear’ causes door seals to become less effective. For these reasons, microwave ovens are a potential source of interference for WPANs. In [18], the received the PER is 12% for the transmitter node to coordinator spacing 6 m and microwave to receiver distance 0.5 m. This influence is becoming more decisive because the number of existing applications based mainly on ZigBee wireless sensor networks operating in the 2.4 GHz band in indoor scenarios is rapidly growing (e.g., home automation and monitoring, energy management, health monitoring and lighting) [19,20]. Recently, mobile technology company Qualcomm has planned to build the methodology to utilize unregulated and unlicensed 2.4 GHz band for mobile [21]. Apart from these interferes Bluetooth and CAM radios are some more devices that operate in ISM band that also affect reasonably [22,23].

In realistic building condition, the radio signal usually encounters some household objects in its endeavor of transmission and experiences further attenuation subject to the absorption characteristics of objects. The propagating electromagnetic signal in the building environment undergoes three primary physical modes that introduce attenuation: reflection, diffraction, and scattering. There are many different objects, including mobile, stationary and transient objects in the indoor environment that causes the loss in RF energy. Higher frequencies attenuate much faster than lower frequencies, similar to free space propagation loss. Path loss, as well as attenuation loss of radio signals, occurs with distance, the amount of attenuation varies with the frequency of RF signal and the obstacle material type and density [24].

Furthermore, attenuation is directly linked with another parameter that is multi-path or direction of arrival (DOA). When an antenna radiates its radio signal simultaneously in all directions, the signal usually takes many paths to reach the receiver. In each path, the signal interact communication environment ambiguously and reaches the receiver with some delay and may be a change in phase and frequency takes place. If the signals received at the

receiver are in phase, then they produce the constructive interference. In case that the signals are out of phase signal, they cause a loss in signal strength as they produce destructive interference. The spread of this delay is known as delay spread, and the attenuation caused by it is called multipath fading. The multipath fading is mainly divided into two parts. First, when the obstacles are large and static, then it is known as large-scale fading, slow-fading, or shadowing. Second, when the obstacles are small and transient, then it is referred to as small scale, fast fading, and scattering. The change in frequency is known as Doppler spreading [25]. In [26,27], they proposed mathematical models with the primary parameters spacing, RSSI and antenna orientation for the indoor environment. Jang et al. [28], presented the wireless sensor network performance metrics for building application, in their study they recorded packet delivery ratio (PDR) 95% for the spacing that was less than 10 m through tick wall at 0 dBm and for the same setup the link quality indication (LQI) was less than 80%.

The direction of arrival measurements offer the best approaches to WSNs localization for the least multi-path loss. Ideally, as we know that wireless communication devices use isotropic low power chip as well as wire whip antenna that radiates radio signal uniformly in all direction equally. A practical antenna does not behave like that. The direction of arrival has a significant role in an indoor environment where system finds different types of obstacles that degrade the performance. The orientation of antenna plays an important role in this. All analysis and characterization of radio communication have been made by the measurements to collect data. This data reveals the nature of EM wave, and with the application of statistical assessment over this data a mathematical model has been generated. The mathematical models are well designed for accurate estimation into the defined laboratory-based environment, but they fail to perform in the realistic environment. Although this model is not purely theoretical, they do not include the real world effect precisely in the mathematical models.

Despite the fact that there are some recent researches available to identify and mitigate the issues of smart building, but these are insufficient and unreliable methodologies. To support the development of desired experimental methods, this research presents the methods and scientific approach that help to describe the main aspects that must be considered.

Our aim is to perform experiments and build the mathematical model that include the real world effects and parameters.

Research presents a realistic approach to getting the optimal performance from smart building monitoring system. We can define the intelligent building monitoring as an application of automation with integral systems of accommodation facilities to boost and progress the everyday lifespan of an occupant. In this research, we have designed an XBee series-2 based intelligent building monitoring system that operates on the ZigBee protocol. Our idea is to generate a system-level design approach to formulating design issues and possible solutions.

The remainder of the article is organized as follows. In Section 2, we initiate with the ZigBee-based smart building environment description. In Section 4, we present the experimental issues based on interference and attenuation losses. Section 5 describes the mitigation and possible suggestion to handle the issues. Lastly, we conclude in Section 6 with the possibility of future work.

2. Description of smart building system

The smart monitoring approach was first implemented in an old house and later it was taken to a building apartment. The smart and intelligent monitoring system is running continuously for the last 18 months without any major problem, in real world condition where it has inhabitants. In the wireless radio communication, we find different types of ZigBee RF modules. For our research application, we selected Digi XBee Series-2 RF. The short description of the smart building system and deployment of sensor nodes is represented by the following parts [29–34].

2.1. Topology and device configuration

ZigBee can be programmed in any of the four possible ways by drivers as well as software. It usually functions in two operating modes; the first is an application programming interface (API), and the other is application transparent (AT). ZigBee Mesh topology is the most preferred topology for the urban environment. Table 1 describes the possible device selections and features [32].

There are some minor safety measures and maintenance requirement that is associated with physical damage and the power supply to sensor nodes.

The design of current sensor deployment inside the smart building is shown in Fig. 1. This layout depicts the sensor location in the real and genuine, smart building,

Table 1
ZigBee device modes and their functions.

ZigBee device type	Function
ZigBee coordinator (ZC)	There is precisely one coordinator for every single network, and this is the device that takes the network establishment responsibility of the network. This coordinator is the transceiver, RF module that not only receives the data from respective sensor nodes connected to it, but also looks for remote configuration and fault detection of other associated sensor nodes in the network
ZigBee routers (ZRs)	ZigBee routers (ZRs) are applied to extend the network coverage area for wireless communication. The ZRs transmit the packet of their neighbor to designated path. The ZED cannot communicate data of other nodes; they are the last end of the network. They only pass their data towards the receiver. They are the source point of data
ZigBee end device (ZED)	The ZED node can convey its data and other neighbor's data as well in the network
ZigBee end-device plus router (ZEDR)	The ZEDR node can convey its data and other neighbor's data as well in the network



Fig. 1. Layout of sensor deployment in the smart building.

Table 2
Technical description and function of sensing units.

Sensor	Technical description and function
Force sensing unit	The flexforce sensor is a Piezoresistive Sensor A301 used to get the amount of pressure applied on any object. When any pressure is forced on the sensor, the resistance of the sensor drops. Eventually, the output voltage rises. The range of resistance varies in force sensor specification found in different types of sensors. The pressure is ideally applied in the central circular portion of the sensor on both borders. The sensor is deployed underneath the objects to sleep and sit upon. The sensor is connected to a conditioning circuit with the 9 V power supply. It is basically analog as well as digital output based sensing unit
Contact sensing unit for domestic objects	For the purpose of household and everyday entities habit monitoring such as a self-grooming table, almirah, and office desk, we designed wireless contact sensing unit and connected them. The designed contact sensing unit connected to household and everyday stuff to identify the frequency of usage, and these objects usage are monitored at local home gateway server by ON/OFF values. It is digital output based sensing unit
Temperature monitoring unit	To design temperature sensing unit, the LM35 IC is connected to conditioning the circuit for ambient temperature monitoring. It is analog output based sensing unit. This sensing unit deployed in indoor and outdoor conditions. Outdoor sensing unit to obtain outside environmental temperature and compare it with indoor value
Movement monitoring unit	The passive infra-red (PIR) movement monitoring unit is designed to identify the motion within the coverage range of the sensing system. This PIR sensing unit is compact, power-efficient, flexible and durable. These sensing units are also known as "IR motion detector". It operates on 5–12 V supply. These are binary mode sensors, and they are interfaced with RF XBee modules. It is digital output based sensing unit. The PIR sensing units are placed at the entry and exit of rooms, kitchen and bathroom
Electronics and electrical appliances monitoring unit	This power usage monitoring and control unit contains a transformer and other circuit components. The transformer block comprises of voltage and current transformers. The step-down voltage transformer is used to transform the mains from 220 V to 10 V signal, and the current transformer ASM010 is used to link the current in the line wire to the load through the current transformer circuit. For signal amplification, operational amplifier LM324 is applied associated with other components such as a rectifier, capacitors and gain resistors of specific parameters. The analog sensor signal output is supplied to the analog channel of radio communication chip for wireless transmission. It is analog output based sensing unit
Food indication unit	A novel approach is proposed and implemented to generate a pattern of eating habits. The push button is integrated with RF module XBee with the help of conditioning circuit

where inhabitants live, and research aims to arrange the sensor nodes towards wellness data reception and forecasting. These heterogeneous sensors include PIR, temperature, force and electronic and electrical appliances monitoring unit, force sensor and food indication button. A quick overview over these sensing units is presented in Table 2.

Figs. 2–5 give the pictures of the sensor unit placement in the smart building to monitor the activity and provide the assisted living for wellness. These heterogeneous sensing units transmit their data through ZigBee end-device to Coordinator. The data to local MySQL server is raw data from which information is extracted through software.



Fig. 2. Electrical and electronics appliance usage monitoring unit.

The software is designed and programmed according to the individual requirement of data extraction. The graphical user interface is designed with the help of visual studio

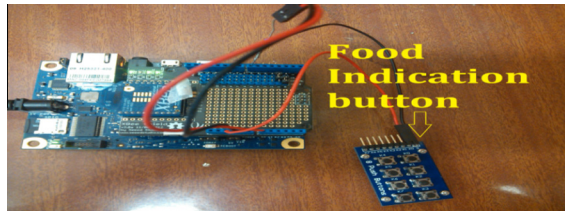


Fig. 3. Food indication button.

C# to upload raw data to MySQL server. From the local server that data will be analyzed with the help of data mining and machine learning algorithm, and uploaded on a designed website via the internet. The local home gateway server is shown in Fig. 6.

3. Methodology to measure interference and attenuation loss

The research approach proposed and implemented in this paper is under a realistic environment with simple and compact components. From a user perspective, the reliability is optimum service delivery, as this optimum performance in service is only possible with the best reliability. So reliability is essential and desired user data should be transmitted, received and analyzed within acceptable and defined time duration in near real time with the best precision value and the least error.

In WSN-based smart home explaining the reliability in system performance, perspective is not easy as pie, because the radio communication system finds some vari-



Fig. 4. (a) The force sensing unit and (b) PIR sensor for activity monitoring.



Fig. 5. Temperature sensing unit.

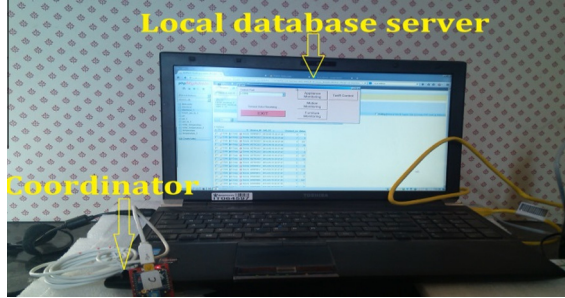


Fig. 6. Home gateway setup.

ables that influence the reliability badly. The most common explanation for reliability is data reliability; data transmission, reception, measured error and delay. The data transmission and reception is the function of communication medium between sensor nodes. The quality of this radio communication link enhances the chances of reliable data delivery. However, the design consideration of the sensor node also decides the performance because they are the source of data, and if data from the source is corrupted, then the system cannot achieve a reasonable accuracy. Most of the time even with good RF link and best sensor node design consideration system get less accuracy. The reason of this is improper routing selection and obstruction in the building environment. The urban environment is full of obstacles, so it causes loss of data. Improper routing and topology increase this data loss more as sometimes an end-device node does not find the nearby router node and that data usually get lost. The signal transmission takes place with the speed of light, so the delay is very small or negligible, although designer need to consider this latency because in smart building designing present system is focusing on real-time intelligence. The combined delay at the sink will be large enough to affect the near real time streaming.

We can better understand this by the packet reliability terms of ZigBee-based WSNs. Packet delivery ratio (PDR), packet success rate (PSR), packet loss rate (PLR), packet error rate (PER), received signal strength, Signal to noise ratio and received packet delay are some of the parameters that define system reliability and performance. To evaluate these parameters in IEEE 802.14.4 ZigBee-based wireless sensor and networks, the smart building setup is developed and implemented on real-time applications. The results show that the distance, deployment environment and positioning of sensor nodes are key parameters that decide the reliability of wireless sensor and networks. For better understanding and system performance evaluation, these parameters have to be formulated with real world effects.

3.1. Latency

In the wireless system, the real-time performance is highly affected by traffic condition, congestion and collision. If the information is sent from the sensing nodes at

a predefined sampling rate, it is supposed that the receiver receives with the same rate. This packet are routed via different communication paths, so they take different time, and some of them may be lost in the endeavor to the destination. There is time out, i.e., the deadline, for these packets' arrival. Hence, one of the major pointers of ZigBee network performance is the packet delay between consecutive packets perfectly received by the Coordinator. To assure the temporal rationality of time-signature, the measurements have to be executed on the same computer system and with the common clock reference.

Digi's XBee Series 2 radio modules run ZigBee 802.15.4 firmware, which allows them to transmit data in a point-to-point, peer-to-peer or point-to-multipoint (star) network architecture. The time it takes to transmit a data packet is a sum of the Time on the Air, an acknowledgment (Time for CSMA-CA and Retries) and propagation time.

Total received delay time (T_{dt})

$$= \text{Time on the air } (T_a) + \text{Time on-air Ack } (T_{ack}) \\ + \text{Time upload } (T_{sci}) + \text{Propagation time } (T_p) \quad (1)$$

T_a = Packet length/ air data rate

$$T_a = \frac{8(B)\{[Sd_b] + n_2[Add_b] + N[Pl_b] + [C_b] + n_1[Pc_b]\}}{Adr_{bs}} \quad (2)$$

T_{ack} = Packet length/ air data rate

$$T_{ack} = \frac{8(B)\{[Sd_b] + n_2[Add_b] + N[Pl_b] + [C_b] + n_1[Pc_b]\}}{Adr_{bs}} \quad (3)$$

T_{sci} = Payload length/serial peripheral interface

$$T_{sci} = \frac{8[B] \cdot \{[Pl_b]\}}{Adr_{bs}} \quad (4)$$

Annotation used above:

B = bit/bytes

Sd_b = starting delimiter

Add_b = address bytes

Pl_b = payload bytes

C_b = cyclic redundancy check bytes

Pc_b = packet control bytes

Adr_{bs} = air data rate in bit per sec.

The propagation delay T_p is the time that it takes a signal to propagate through the communications media from a node to the next node. It can be computed using the following equation. Here, D is the distance from the node to the next node and S is the propagation speed of the media. The speed of wireless signal propagation is equal to the speed of light.

$$T_p = D/S \quad (5)$$

The latency calculated from Eq. (1) includes some overheads caused by the computational and communications systems and controllers. To minimize the jitter, it is recommended to limit the processing load on the computer. The jitter is a complex problem mainly related to the wireless networks and infrastructure. This delay is closely linked to inter-packet delay. Inter-packet delay is the degree of the inconsistency over the communication time of the

latency across a wireless network. One of the possible solutions is to introduce the jitter buffer to queue up the received message. In the smart building-based wireless network, instead of introducing jitter buffer between network and converter, it can be done by utilizing the RAM efficiently. This reduction in load results in terms of availability of RAM for packet transmission and reception without I/O operations blocking.

3.2. Packet delivery parameters

The packet sent from the source node must be received at sink node without any distortion and manipulation that affect the accuracy. This is usually determined by the number of messages sent from the source and received at the destination. The experiments are executed by regularly transmitting and receiving packets from the transmitter (mostly wireless sensing modes) Tx to receive (coordinator) Rx.

PDR, PSR, PER, and PLR are closely linked to the packet reliability and system performance, and they represent the packet accuracy at a different level.

- PDR: Packet delivery ratio is the number of packets received at coordinator to the number of packets sent from the transmitter. It is represented in percentage.

$$\text{PDR (\%)} = \frac{N_r}{N_s} * 100 \quad (6)$$

N_r = Total number of packets received by the coordinator from an end-device.

N_s = Total number of packets sent by the end-device.

The more the PDR value, the better the accuracy.

- PSR: Packet success rate is the number of packets successfully received without any error to the number of packets received at the coordinator. It is represented in percentage.

$$\text{PSR (\%)} = \frac{N_{we}}{N_r} * 100 \quad (7)$$

N_r = Total number of packets received by the coordinator from an end-device.

N_{we} = Total number of packets received by coordinator without error from an end-device.

The more the PSR value the better the accuracy.

- PER: Packet error rate is the function of the number of packets successfully received and the number of packets received at coordinator. It is represented in percentage.

$$\text{PER (\%)} = \frac{N_r - N_{we}}{N_r} * 100 \quad (8)$$

N_r = Total number of packets received by the coordinator from an end-device.

N_{we} = Total number of packets received by coordinator without error from an end-device.

The less the PER value the better the accuracy.

- PLR: Packet loss rate is the function of the number of packets received at coordinator and the number of packets sent from the transmitter. It is represented in percentage.

$$\text{PLR (\%)} = \frac{N_s - N_r}{N_s} * 100 \quad (9)$$

N_r = Total number of packets received by the coordinator from an end-device.

N_s = Total number of packets sent by the end-device.

The less the PLR value the better the accuracy.

3.3. Link quality metrics

Electromagnetic interference is the disruption that upsets desired node signal processing through electromagnetic radiation emitted from an external source. ZigBee-based sensor nodes operate in the 2.4 GHz ISM spectrum. The causes of disturbance in this frequency band include:

- Bluetooth (IEEE 802.15.1)
- Wireless USB version 2 (IEEE 802.15.3)
- WI-Fi (IEEE 802.11)
- Microwave ovens
- Other sources, like some cordless phones and RF motion detectors.

The effect of this disturbance can be examined by received signal strength, LQI and signal to noise ratio.

3.3.1. RSSI

Received signal strength indicator (RSSI) is the signal strength level of the RF end-device measured in $-\text{dBm}$ (for isotropic antenna) of a particular packet, received at the local home gateway coordinator. The detected signal strength value reduces with increase in spacing between transmitter and receiver and path loss effect. Additionally signal quality is affected by other RF devices operating in ISM band. If the transmitting node has a transmit power of P_t watts and this antenna power in the logarithmic domain is expressed in dBm (in mW), with an isotropic antenna gain of G_t dBi, then the total effective isotropic radiated power (EIRP) is $P_t * G_t$. So received signal at receiver is given by

$$P_r = P_t + G_t + G_r - PL \quad (10)$$

G_r is the receiver antenna gain, and PL is the joint path loss parameter that includes attenuation due to path losses.

In the building environment, the path loss is represented by

$$PL = L_{js} + L_{sf} + L_{ff}(t) \quad (11)$$

Here L_{fs} is the term for free space line-of-sight path loss, L_{sf} loss is due to slow fading caused by large static obstructions like a wall, and L_{ff} loss is the small-scale fast fading loss that occurs due to destructive interference from multipath effects. This is the primary and most significant loss in the building environment. This loss varies with time t . Most of the times in the building environment electromagnetic signal does not find the LOS between transmitter and receiver, so it travels by multipath or in non-line-of-sight. Minimum acceptable SNR value $\text{SNR}_{P(T,R)}$ should be greater than the threshold value η to recover the transmitted signal. The value of η is defined by multiple experiments and measurement in that particular environment.

$$\text{SNR}_{P(T,R)} = \text{SNR}_{\text{Pref}} - 10\beta \log \left\{ \frac{(d(T,R))}{d_{\text{ref}}} \right\} + X_{\sigma} + \alpha(T,R) \quad (12)$$

Propagation loss estimation in a building environment shows that the average received signal strength at any point in the network decays as power law of distance d (T, R) between a transmitter and a receiver. SNR_{Pref} is the power received at a close reference point in the small reference distance d_{ref} from transmitting node and β is the path loss exponent. X_{σ} is zero-mean Gaussian distributed random variable with standard deviation σ in dBm, for long term variability consideration, which is used to approximate the fading phenomenon in building environment. $\alpha(T, R)$ = attenuation in dB per unit distance which varies according to material and obstruction type. The term $\alpha(T, R)$ and β must be determined in each wireless network individually.

An isotropic antenna is known for radiating the power uniformly in all directions (in a sphere), which is only possible in theory and does not exist in actual practice. The direction of arrival of the signal at receiver become significant in the building environment where wireless sensing system finds obstructions and interference sources. There is a direct relationship between the direction of a signal and the associated received steering vector. In actual practice, defining and evaluating the DOA is complicated because there are an unknown number of RF signals striking on the receiving antenna concurrently, each from unidentified directions and with unknown amplitudes. Additionally, the received RF signals are always degraded by the disturbance caused by noise, attenuation, and interference.

$$P(T, R) = P_R + \sum_{j=1}^N P_{ij} \cos(\theta_j + \alpha_i) + \sum_{j=1}^M P_{pj} \cos(\theta_j + \beta_p) \quad (13)$$

P_R = Peak or reference received power value at coordinator.

P_{ij} = Power affected by interference sources, j is number of interference sources. It is $1-N$.

P_{pj} = Power affected by multi path fading, j is number of multi path loss sources or multi path fading level. It is $1-P$.

θ_j = Angle of arrival with respect to interference sources.

α_i = Phase change caused by interference sources.

β_p = Phase change caused by multi path fading.

3.3.2. Signal to noise ratio (SNR)

The other devices, which are operated in ISM band, cause disturbance to desired RF signal. These undesired disturbance sources produce RF power that interrupt the required signal for smart home operation. This is ultimately referred to as noise.

$$\text{SNR} = \frac{P_{\text{Signal}}}{P_{\text{noise}} + P_{\text{interference}}} \quad (14)$$

$$\text{SNR (dBm)} = P_{\text{Signal}} - P_{\text{noise}} - P_{\text{interference}} \quad (15)$$

4. Experimental observations and prediction

4.1. Fundamental tests: Packet delivery parameters (PER, PLR, PSR, and PDR) and link quality parameters as a function of spacing

These are the native tests to understand the performance of the wireless sensors and networks in the smart building environment, with least interference. All the experiments and setup have been developed to generate the plots for each metric as a function of distance. The sensing nodes are deployed in the smart building, and spacing between the nodes has been varied. For every plot, we have collected and analyzed 5000 plus sample values to define the uncertainties precisely. The transmitter power is set at 2 mW (+3 dBm) boost mode, and the receiver sensitivity is -96 dBm.

The sensor node arrangement for hop distance effect analysis experiment has been given in Fig. 7. Fig. 8 shows how the delay in the wireless communication varies with hop distance. Hop1 means the packet is sent without any router device, while hop2 represents the packet is sent with one router between the end device and coordinator. Similarly, hop3 and hop4 show the packet is sent via 2 and 3 router devices between the end device and coordinator, respectively. In hop1 we have varied the spacing between Transmitter-end-device (Tx) and Receiver-coordinator (Rx). Whereas in hop2, hop3 and hop4 we kept the end-device and coordinator at a defined distance and

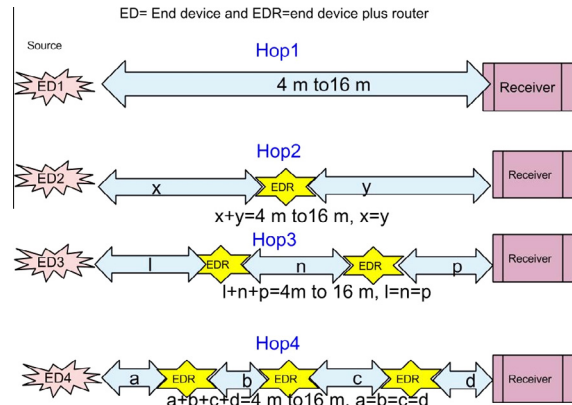


Fig. 7. The experimental sensor organization for hop distance effect assessment.

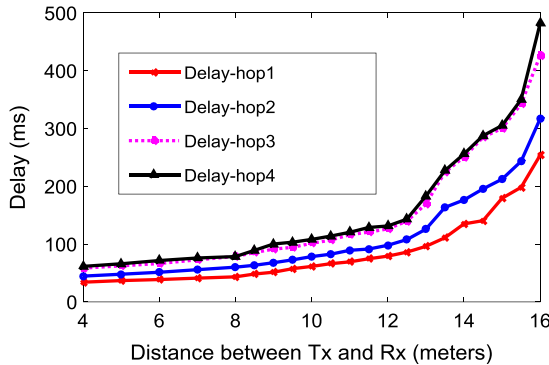


Fig. 8. Delay as a function of hopping distance.

varied the routers spacing with respect to end-device and coordinator. The other devices that we have used as the router in hop2, hop3 and hop4 are router-end-device. The delay has increased with the increase in the spacing between source and destination. Additionally, the delay affects more when a WSNs use number of hops. Every time the end-device (ED) delivers the packet to end-device-router (EDR) in the case of multi-hop communication and this EDR keeps its own packet delivery at the highest priority. If EDR generate its own packet P1 and at that same moment it receives relay packet P2 from another neighbor node, then it will deliver P1 followed by P2. This results in the latency. The estimated uncertainties in delay are 27 ms based on the standard deviations of multiple investigations. Although the delay value that server has recorded is in milliseconds, it has the potential to change the real-time application to near real-time application. The smart building solution offers the real-time monitoring through the website from a remote distance. The whole setup is the WSNs based realistic, smart building environment where some of these sensors are event based, and the rest have fixed sampling rate. The length of the packet varies from 20 to 24 bytes.

Fig. 9 shows the PDR values of all four different setups, in all cases, PDR decreases with increase in spacing. In three cases PDR drops in PDR3, 2 and 1, except PDRhop4 where we have used 3 EDRs. In PDRhop1, the drop is quite significant where it starts decreasing after 8 m followed by

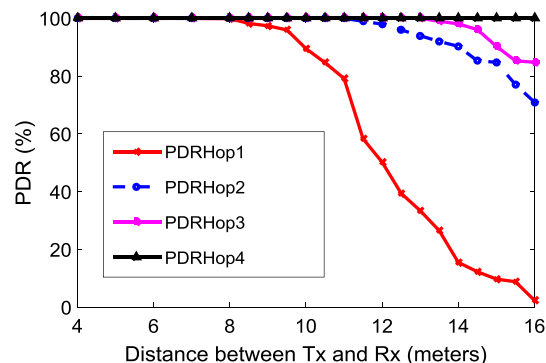


Fig. 9. PDR as a function of hopping distance.

PDRhop2 after 12 m and followed by PDRhop3 after 14 m. The estimated uncertainties in PDR are 1% based on the standard deviations of multiple investigations.

Fig. 10 shows the PER values of all four different setups, in all cases PER increases with increase in spacing. In all four cases, PER raises significantly after the spacing 8 m. In PERhop1, the drop is quite major where it starts increasing followed by PERhop2. While PERhop4 has least affected followed by PERhop3. The estimated uncertainties in PER are 1.37% based on the standard deviations of multiple investigations.

With increasing in spacing between Tx and Rx the packet delivery performance degraded so a better solution is to deploy EDR to improve it.

4.2. Analytical and parametric tests

The experimental strategy is developed to assess the effect of various parameters on packet delivery parameters (PER, PLR, PSR, and PDR) and link quality parameters. The issues investigated in this research work are as follows:

1. Multipath fading and spacing between Tx and Rx (S_{Tx-Rx});
2. IS and spacing between IS and Rx (S_{IS-Rx}), and IS and Tx (S_{IS-Tx});
3. The direction of arrival (DOA) in relation with IS to the line-of-sight and multipath fading. Additionally, the angle between Rx and IS (θ) is considered;
4. Communication channels.

The aim of these tests is to evaluate effects of different issues on the performance of WSN for smart building. Table 3 presents the issues and the range of tests. In IS, research work has considered most common sources of disturbance in ISM band. In the endeavor to find the least affected channel with Wi-Fi, we selected 15, 25 and 26. The distance between the ED and coordinator is kept from 2 m to 16 m, which is sufficient to consider one floor of the building apartment. To observe the effect of IS on received signal, the spacing between IS and Rx varied from .5 m to 5 m. This effect has been recorded for line-of-sight and multipath fading environment.

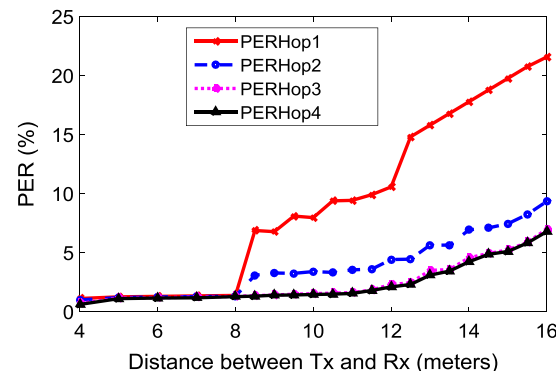


Fig. 10. PER as a function of hopping distance.

Table 3

The issues and their range in the experiments.

Synod	Issues	Range
1	Interference sources (IS)	Wi-Fi, Bluetooth, Microwave, cordless phone
2	Communication channel	15, 25 and 26
3	S_{Tx-Rx}	2–16 m
4	S_{Is-Rx}	.5–5 m
5	Deployment angle of IS with respect to Tx-Rx line of sight	0–360°
6	Multipath fading materials by attenuation source (AS)	Glass (GLS), plywood (PYWD), metal (MTL), concrete (CNCRT), brick (BRCK), coated glass (CTDG)
7	Separation S_{Tx-AS}	.5–6 m

The antenna chip/wire/whip are isotropic antennas so the direction of arrival of a signal and their location with respect to receiver and IS should not affect the performance ideally. In actual practice, we have observed that the location and DOA have considerable consequences. In the experimental setup, the IS kept at different location and angle from 0° to 360°. The living environment contains heterogeneous sensors, and the deployment of these sensing units is decisive to get optimum received signal value. The building is made of different materials and contains various household objects (steel chair, metal table, etc.) which cause the attenuation loss to low-power wireless communication. This research study includes all possible source of attenuation that degrades the signal characteristics.

4.3. Smart building attenuation

Metrics of smart building WSNs are examined to mitigate the losses and generate tradeoff in the deployment environment. WSNs offer remarkable prospects for effective utilization of power and enrichment in inhabitant wellbeing in the buildings environment by improving the communication link quality to make sensing data available all the time. A major issue in the implementation is the ambiguity between designers concerning the consistency of wireless communication links via building material and household objects location. Tests have been done to investigate the RSSI and packet delivery parameters values as a function of transmitter–attenuation source separation S_{Tx-AS} distance and obstruction type. These experiments are implemented through packet reliability, the realistic switch from consistent to inconsistent wireless communications at different distances and materials. The packet delivery rate is measured in the realistic building; the RSSI is interrelated with the packet success rate in the fairly uncontrolled noise environment. These tests are carried out in last year, with 5000 plus samples analyzed in each test. **Table 4** shows the independent constraints varied in the experiments.

For this particular test, we have picked the fixed sampling rate of 5 ms and packet size is 22 bytes. The distance between STx and Rx has been kept 8 m fixed, and the separation between obstructions to transmitter varied from

Table 4

Obstruction-material details of building environment (Different kind of obstacles a radio signal passes through in smart home environment).

S. No.	Material	Thickness	Remark
1	Plywood as well as wood	2.3 cm	Doors as well as divider
2	Metal mostly steel/iron	1.2 cm	Doors, tables, bed and chairs, interior office panel
3	Concrete	27.5 cm	Wall
4	Brick	29.3 cm	Wall
5	Glass and coated glass	1.2 cm* and 1.7 cm	Window* and doors, divider

.5 m to 6 m. **Fig. 11(a)** presents the smart building experiment layout. The tests have been done in various obstructions conditions that we get in the smart building to examine the adverse effect of plywood, metal, concrete, glass, coated glass and brick on the wireless signal multipath fading. The effective area of obstructions is varied so our approach is to deploy transmitter such that it can offer best measures of effects. All the obstacles are part of the building environment. There is nothing we choose from the outside environment to perform the test.

The experiment carried out in the open field as well as the controlled environment is repeatable, and designer can estimate and analyze with small scale data sets. The building environment introduces ambiguity and to generate accurate results from analysis and observation all the possible consideration of dependent and independent variable have been made. **Fig. 11(b)** shows the average RSSI values as a function of various genuine obstructions, and the separation between Tx and AS varied from .5 m to 6 m. The measured standard deviation (σ) is ± 3 dBm. Less the separation between Tx and AS poor the RSSI value, Metal has caused the major degradation in signal propagation. From .5 m to 3 m there in the presence of metal AS the RSSI from -104 dBm to -96.81 dBm that is not good enough to recover packet from it. The plywood and wood are least affecting AS followed by Glass, followed by brick and concrete and followed by coated glass. Up to $S_{Tx-AS} = 1.5$ m, the RSSI for AS glass, coated glass, brick and concrete was less than the threshold sensitivity level of the receiver. With the spacing $S_{Tx-AS} \geq 2$ m, the RSSI improved significantly in the glass, coated glass, brick, and concrete.

Fig. 12(a) and (b) shows the PDR data. The graphs represent that the nearly all AS PDR values have secured 93% plus except metal AS for the spacing $S_{Tx-AS} \geq 2$ m. With the increase in S_{Tx-AS} value, the PDR values in all AS have been improved considerably. The PDRMETAL has recorded 90% beyond $S_{Tx-AS} = 3$ m. There is a slight difference in the PDR metrics of glass, plywood concrete, and coated glass. The major improvement in PDR with an increase in separation is in plywood, followed by the glass, followed by brick and followed by concrete and coated glass. The reliable range of communication in the glass, plywood concrete, and coated glass is $S_{Tx-AS} \geq 2$ m, while metal is an exception. The measured standard deviation (σ) for PDR is 2%.

Fig. 13(a) and (b) follows the same trends we find in PDR. Except the PSRMETAL, the rest have touched 96% plus

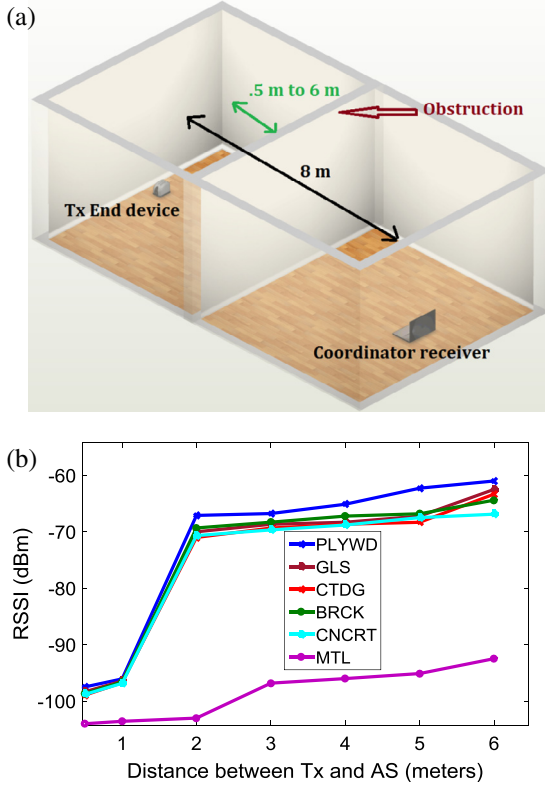


Fig. 11. (a) Layout of attenuation loss test, (b) RSSI as a function of different building materials, where $S_{\text{Tx-AS}}$ is varied from .5 m to 6 m.

for spacing $S_{\text{Tx-AS}} \geq 2$ m. The measured standard deviation (σ) for PSR is 1.5%.

Despite the large uncertainty in the recorded data, we have identified some trends. The wood, plywood, and glass cause little disturbance to the wireless signal propagation, and this also justified by the low dielectric constant values of these materials. Our approach has been to evaluate the possible ways to avoid unreliable communication as well generate tradeoff to get optimum packet reliability parameters. Table 5 shows the optimum values for various attenuation sources.

4.4. Direction of arrival (DOA)

These tests demonstrate how the direction of arrival (DOA) can help to get best signal performance as a function of IS. In the presence of IS, we do not get optimum signal performance that is highly essential for packet reliability. When we place IS, it influences and causes loss to the desired wireless signal. This loss comes in terms of packet loss as well as an error. Our aim is to investigate the possible approach and methodology to mitigate it.

For this test, we arranged one wireless transmitter and one receiver coordinator. Various IS sources are deployed and their spacing from receiver have been varied. Moreover, the angle between the Tx-IS and Rx-IS have been varied to discover the best possible deployment angle in the particular environment. Fig. 14 presents the schematic

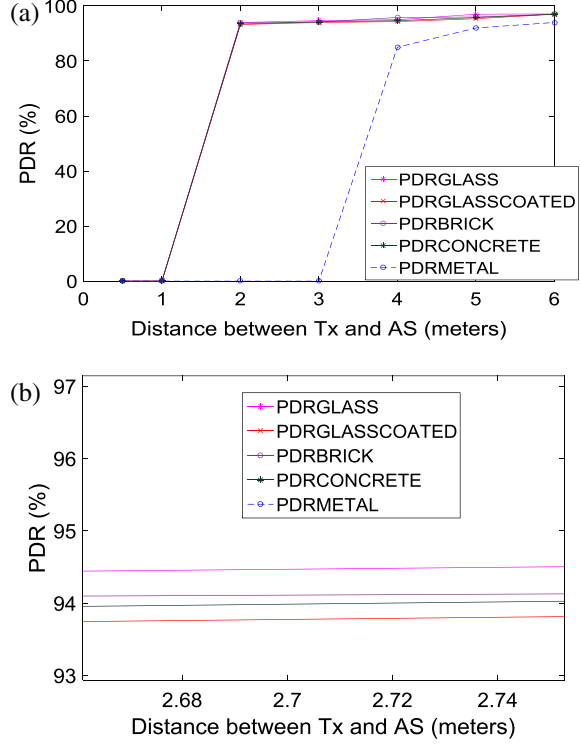


Fig. 12. (a) PDR as a function of different building materials, where $S_{\text{Tx-AS}}$ is varied from .5 m to 6 m and (b) close-up view PDR as a function of different building materials, where $S_{\text{Tx-AS}}$ is varied from .5 m to 6 m.

setup of DOA measurement. We have implemented these tests in two different setups. The first setup is for the line-of-sight and the second setup is for multipath fading. These two experiments are performed for three different spacing $S_{\text{Rx-IS}} = 1$ m, 2 m and 3 m. Additionally, in every experiment either Tx or Rx angle is varied as a function of IS location. In line-of-sight, the desired wireless signal is majorly affected by IS interference while in multipath the wireless signal is affected by AS and IS. The RSSI values are received for three different locations of IS as a function of Rx. Pri represents the RSSI value when the Rx angle has been varied with respect to IS while Ptr shows the RSSI value when the Tx angle changed with respect to IS location.

Fig. 15 presents the RSSI values as a function of the angle between Rx and IS in line-of-sight setup, where the spacing between Tx and Rx is fixed at 3 m. The RSSI values have been recorded for three spacing Pri1 (when Rx is 1 m from IS), Pri2 (when Rx is 2 m from IS) and Pri3 (when Rx is 3 m from IS). In the particular test the peaks in RSSI values have been achieved at 60°, 150°, 240° and 330°. For the same angle, PDR and PSR values as shown in Figs. 16 and 17 respectively have touched peak. The more the spacing between Rx and IS, the less the interference effect on desired wireless signal, and the better the signal performance and packet reliability. Pri3, PSR3 and PDR3 have shown the best results while Pri1, PSR1 and PDR1 have been the worst. The highest RSSI value has been recorded at 60° which is -94.01 dBm and packet metrics PDR is

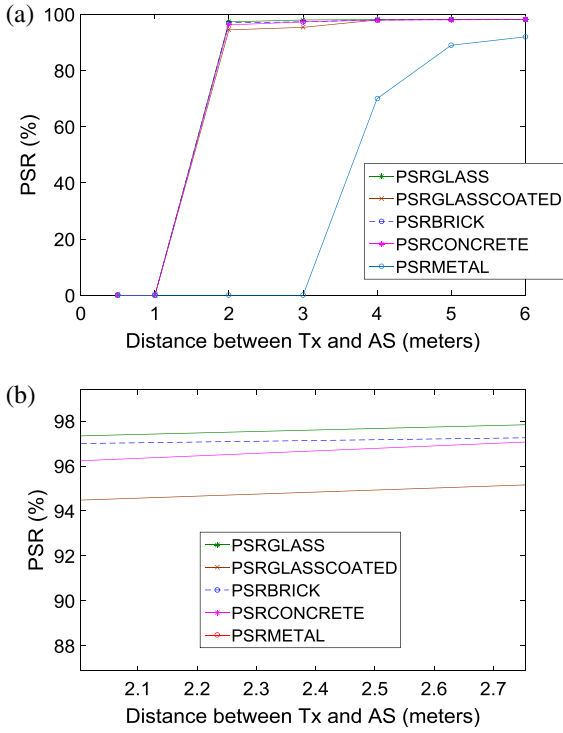


Fig. 13. (a) PSR as a function of different building materials, where S_{Tx-AS} is varied from .5 m to 6 m and (b) close-up view PSR as a function of different building materials, where S_{Tx-AS} is varied from .5 m to 6 m.

87.46% and PSR is 76.28%. The measured standard deviation (σ) for RSSI is ± 1 dBm, PDR is 2% and PSR is 1.5%.

Fig. 18 presents the RSSI values as a function of the angle between Tx and IS in line-of-sight setup. In the particular test the best possible RSSI values have been achieved at 60°, 150°, 240° and 330°. For the same angle PDR and PSR values in Figs. 19 and 20 respectively have attained high values. Similar trends of IS and Rx spacing have been recorded in these graphs as well.

The highest RSSI value has been recorded at 60° which is -94.04 dBm and packet metrics PDR is 86.35% and PSR is 75.29%. The measured standard deviation (σ) for RSSI is ± 1 dBm, PDR is 2% and PSR is 1.5%.

Fig. 21 presents the RSSI values as a function of the angle between Rx and IS in multipath setup, where the spacing between Tx and Rx is fixed at 5 m, and there are some obstacles in between them. The RSSI values have been recorded for three spacing Pri1 (when Rx is 1 m from IS), Pri2 (when Rx is 2 m from IS) and Pri3 (when Rx is 3 m from IS). In the particular test, the peak in RSSI values has been achieved at 45°, 120°, 210° and 330°. For the same angle, PDR and PSR values in Figs. 22 and 23 respectively have touched high values. The highest RSSI value has been

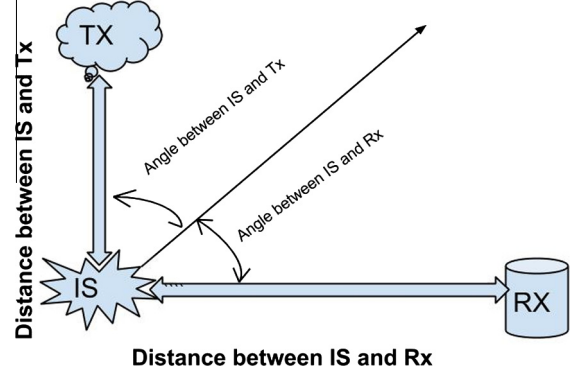


Fig. 14. Schematic setup for IS location for DOA.

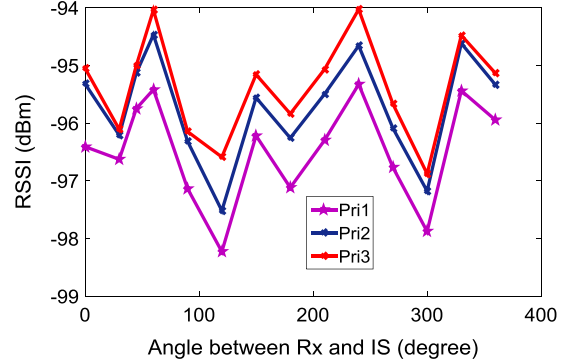


Fig. 15. RSSI as a function of the angle between Rx and IS in the line of sight, $S_{Tx-Rx} = 3$ m.

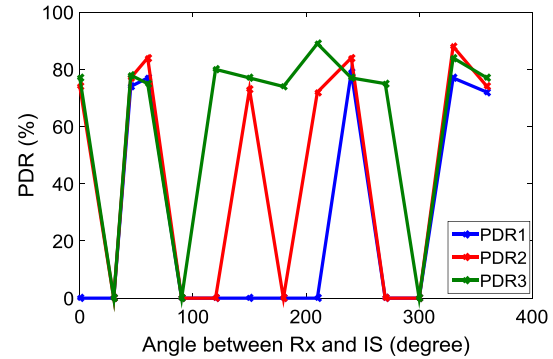


Fig. 16. PDR as a function of the angle between Rx and IS in the line of sight, $S_{Tx-Rx} = 3$ m.

recorded at 210° which is -94.61 dBm and packet metrics PDR is 80.21% and PSR is 71.18%. The measured standard deviation (σ) for RSSI is ± 1 dBm, PDR is 2%, and PSR is 1.5%.

Table 5

Optimum value recorded at $S_{Tx-AS} = 6$ m.

Parameter at distance 6 m	Plywood	Glass	Glass ctd	Brick	Concrete	Metal
RSSI	-61	-62.49	-63.32	-64.4	-66.88	-92.47
PDR (%)	97.55	97.11	97	97.02	97	94
PSR (%)	98.15	98.15	98.15	98.15	98.15	92

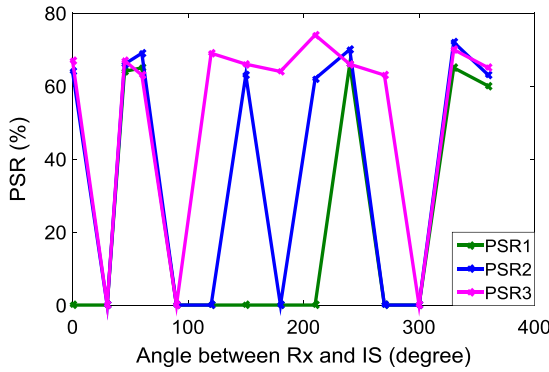


Fig. 17. PSR as a function of the angle between Rx and IS in the line of sight, $S_{Tx-Rx} = 3$ m.

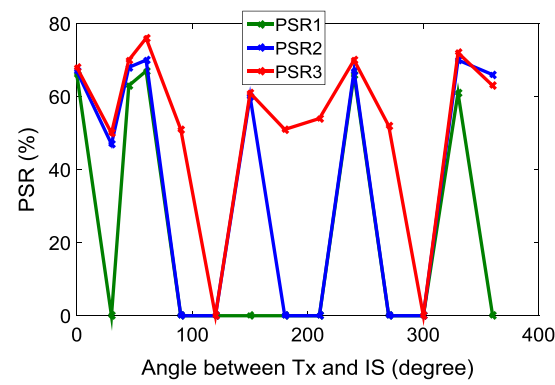


Fig. 20. PSR as a function of the angle between Tx and IS in the line of sight, $S_{Tx-Rx} = 3$ m.

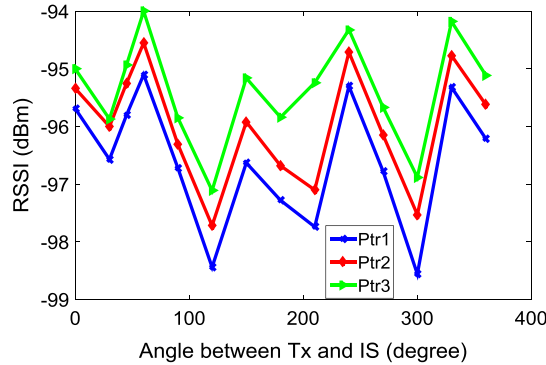


Fig. 18. RSSI as a function of the angle between Tx and IS in the line of sight, $S_{Tx-Rx} = 3$ m.

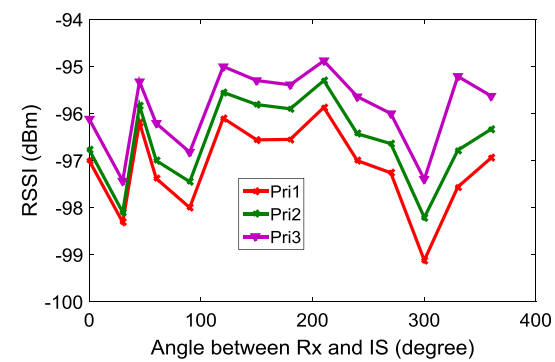


Fig. 21. RSSI as a function of angle between Rx and IS in multipath fading, $S_{Tx-Rx} = 5$ m.

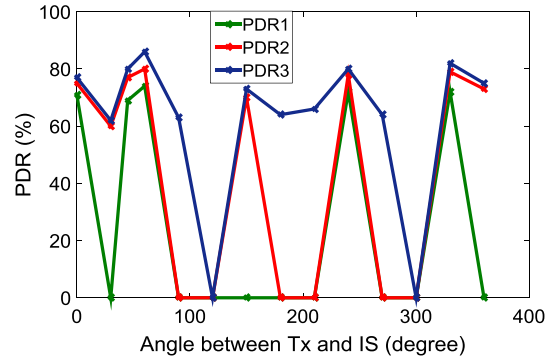


Fig. 19. PDR as a function of the angle between Tx and IS in the line of sight, $S_{Tx-Rx} = 3$ m.

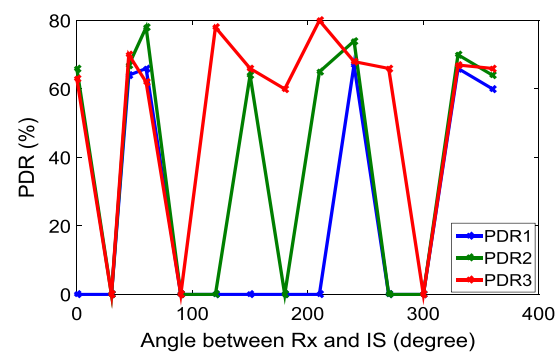


Fig. 22. PDR as a function of angle between Rx and IS in multipath fading, $S_{Tx-Rx} = 5$ m.

Similar trends were found in Fig. 24 that presents the RSSI values as a function of the angle between Tx and IS in multipath setup. In the particular test the peak in RSSI values has been achieved at 45°, 120°, 270° and 330°. For the same angle, PDR and PSR values in Figs. 25 and 26 respectively have touched high values.

Through these tests of DOA, we have discovered that direction of arrival of signal and spacing between receiver

and IS plays a significant role when the potential interference affects the radio communication.

IEEE 802.11b/g, Bluetooth, IEEE 802.15.4, 2.4 GHz frequency hopping spread spectrum portable phones and numerous proprietary wireless technologies operate in the ISM band. The coexistence of different technologies with ZigBee has been captured using the exceptional and economical Wi-Spy tool and displayed using the Chanalyzer package. The channel numbers along the bottom

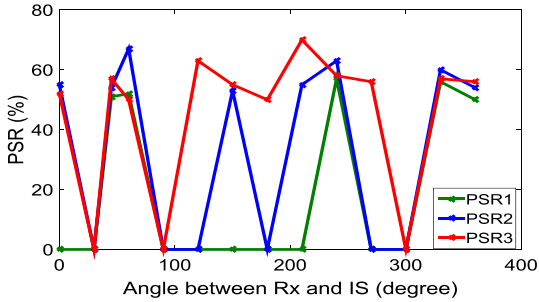


Fig. 23. PSR as a function of angle between Rx and IS in multipath fading, $S_{Tx-Rx} = 5$ m.

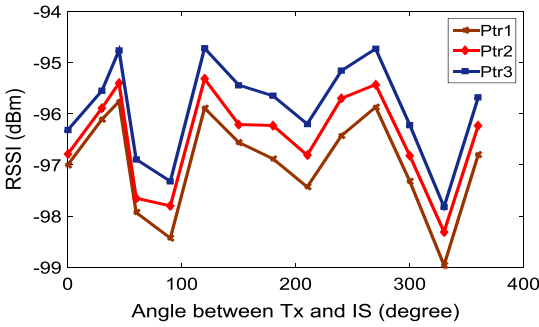


Fig. 24. RSSI as a function of angle between Tx and IS in multipath fading, $S_{Tx-Rx} = 5$ m.

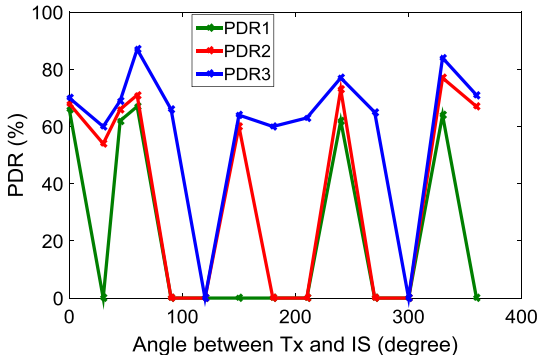


Fig. 25. PDR as a function of angle between Tx and IS in multipath fading, $S_{Tx-Rx} = 5$ m.

are ZigBee channels. We used MetaGeek Spectrum Analysis Wi-Spy DBx & Chanalyzer 5 device as a frequency spectrum analyzer, and configured it for a particular application requirement [35–37]. We are using Density and waterfall graphs to visualize he interference and loss caused by other RF device in ISM band. These graphs represent the RSSI values at different ZigBee channels.

The Density View graph shows what is presently happening in the spectrum, so you can recognize devices, see how loud they are, and see how often they are transmitting. With ‘Color by Utilization’ enabled, the height of the graph shows how loud devices are (amplitude), and the intensity of the color shows how often signals are

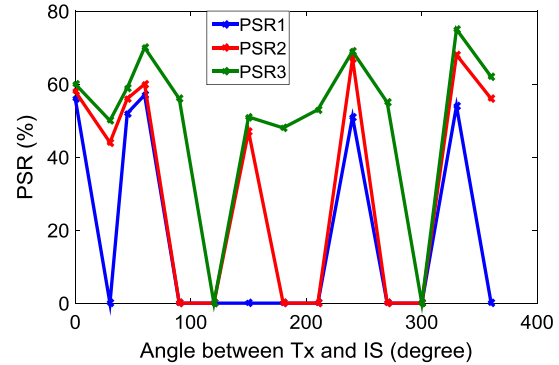


Fig. 26. PSR as a function of angle between Tx and IS in multipath fading, $S_{Tx-Rx} = 5$ m.

occurring. The more concentrated the color, the more often the frequency is in use. This is called utilization, which is analogous to duty cycle and airtime usage. For example, if the frequency has 40% utilization, it is only free for use by other transmitters for 60% of the time. A blue spike or profile shows a short signal, like a clap. A red spike or shape shows a long, unbroken signal, like an air horn. Colors and their significance are as follows: Blue – Less than 10% utilization, Green – 20% utilization, Yellow – 40% utilization, Red – Over 50% utilization

The Waterfall View graphs amplitude over time for all frequencies in the selected band, much like a seismometer graph for earthquakes. This view is useful for watching the spectrum over time. Unlike the Density View, which uses Color by Utilization, the intensity of the color in the Waterfall view shows amplitude. Blue indicates low-amplitude signals, while red indicates high-amplitude signals.

Fig. 27 shows the ZigBee-based system operating at channel 15 without any potential source of interference. **Figs. 28–30** show the interference caused by other wireless technology in smart home monitoring ZigBee channel.

Our ZigBee-based WSNs are functioning at channel 2.430 GHz. The sensor nodes are deployed in Mesh topology into a smart building with spacing between nodes up to 6 m, and the Wi-Fi, Bluetooth and microwave sources are placed at 2-m distance from the receiver (coordinator). Figures show the density and waterfall views of XBee smart building system that is operating at frequency 2.430 MHz under the least interference condition. **Fig. 28** shows the Wi-Fi operation that affected the XBee operation badly. **Fig. 29** shows the Bluetooth functioning over the same frequency of 2.430 MHz, which corrupted the XBee RF link quality. **Fig. 30** represents microwave oven signals dissipate across the whole ZigBee spectrum and spoil the signal performance and packet delivery notably. This interference effect can be better understood by packet reliability parameters, shown in **Figs. 31 and 32**. The packet reliability metrics are most affected in microwave oven followed by Wi-Fi, then by Bluetooth. Bluetooth has the least effect.

Fig. 33 shows the level of degradation caused by different factors. The RSSI value has been majorly affected by S_{IS-Rx} , followed by material attenuation, followed by S_{Tx-Rx}

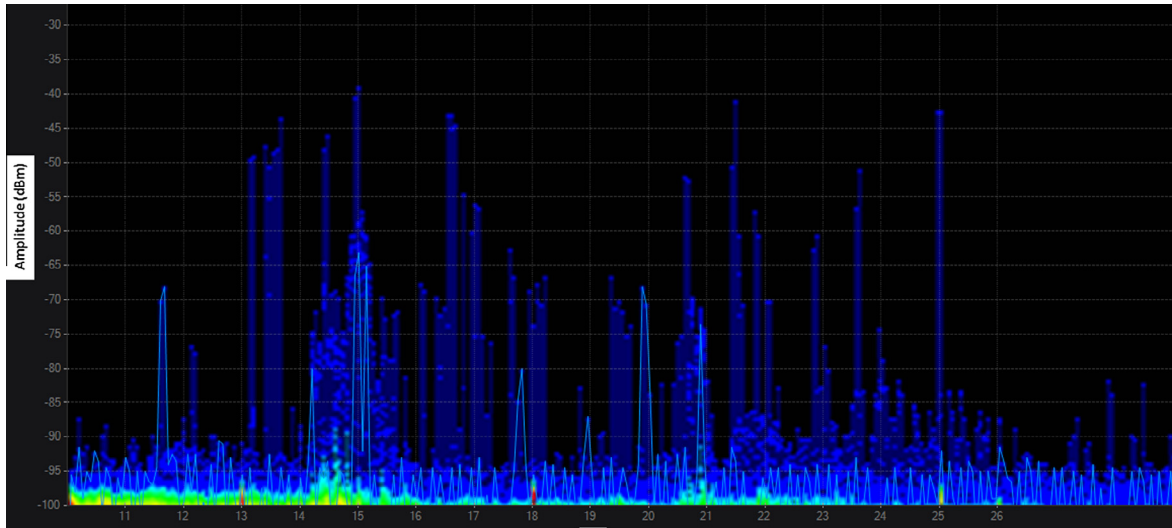


Fig. 27. The XBee smart building system is operating at frequency 2.430 MHz.

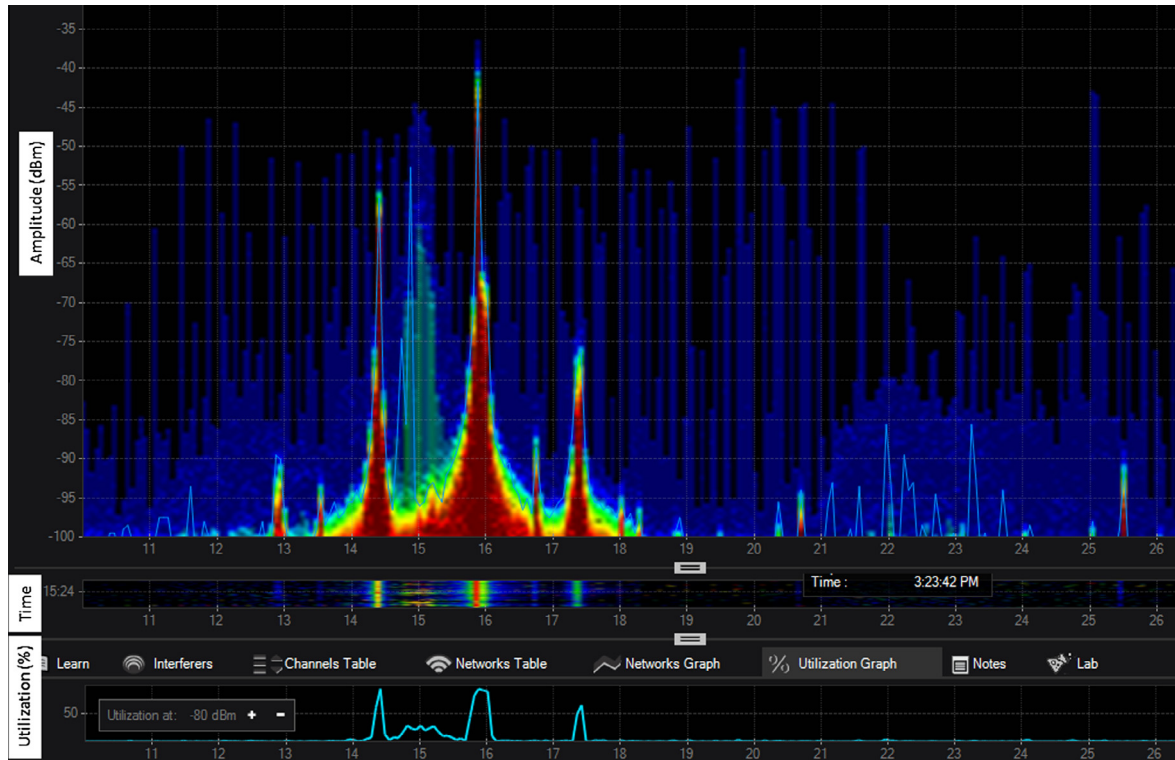


Fig. 28. The Wi-Fi functioning over the same frequency 2.430 MHz, which degraded the XBee RF link quality.

and followed by DOA. The selection of channel has least affected the RSSI value. Fig. 34 presents the effect of different factors on packet reliability metric PSR. Similar to RSSI, the PSR metric is most affected by the S_{IS-Rx} , followed by S_{Tx-Rx} , followed by S_{Tx-Rx} and followed by channel selection. The DOA has least affected the PSR.

5. Mitigation of interference and suggestions

Primarily the IS signal was applied at 2400 MHz frequency, and the corresponding SNR value for ZigBee network was measured. However, as IS signal operating frequency was moving close to ZigBee network operating

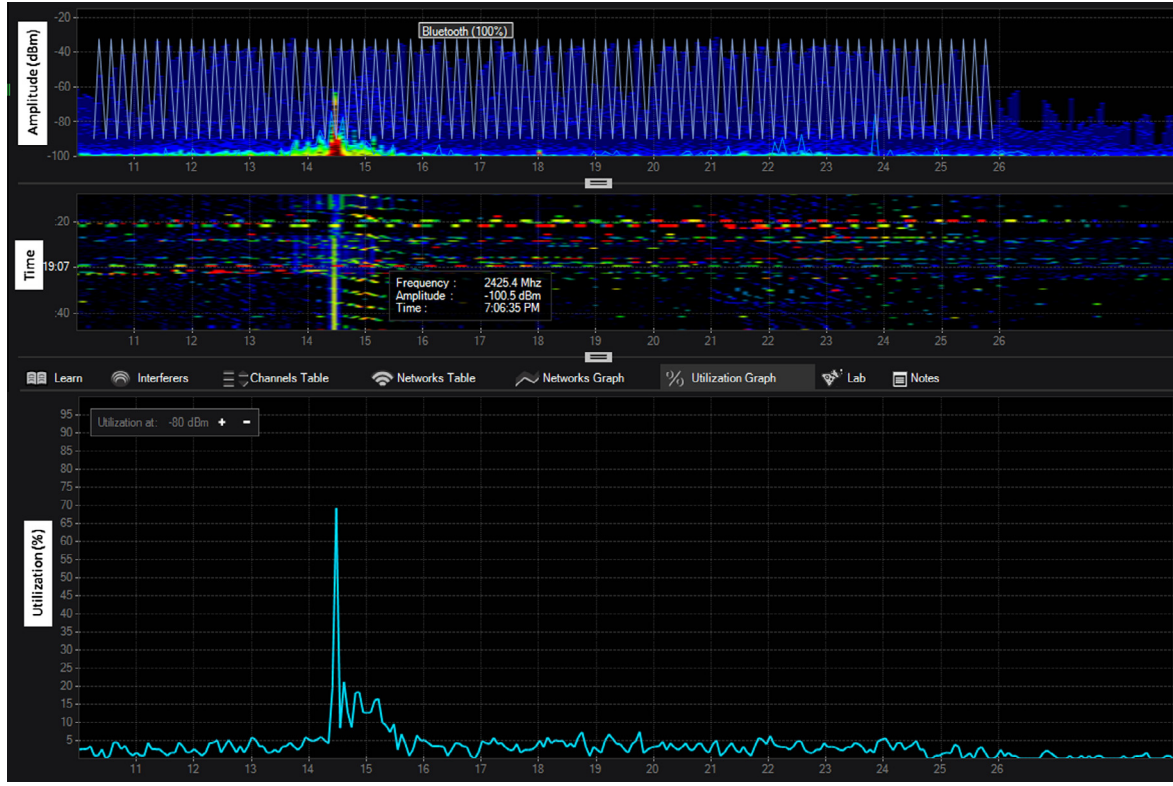


Fig. 29. The Bluetooth functioning over the same frequency 2.430 MHz, which degraded the XBee RF link quality.

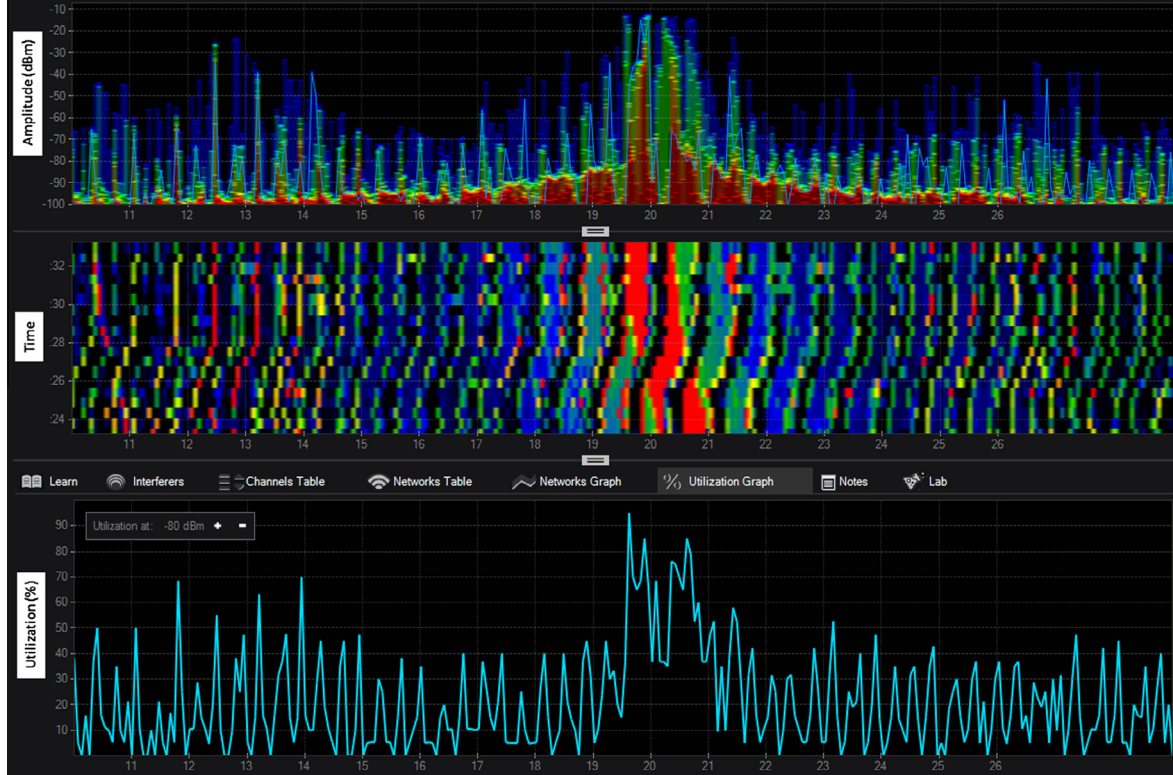


Fig. 30. Microwave oven distributed all ZigBee channels, and the microwave signal are dissipated across the whole ZigBee spectrum.

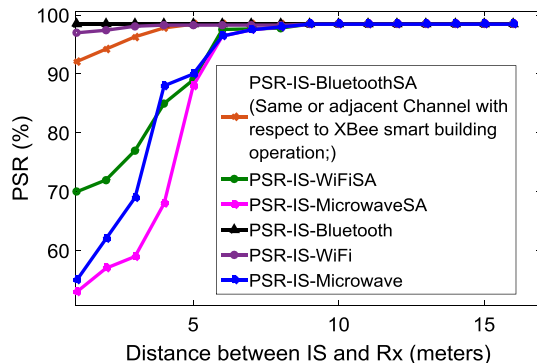


Fig. 31. PSR as a function of the distance between IS and Rx, $S_{IS-Rx} = 1\text{--}16\text{ m}$.

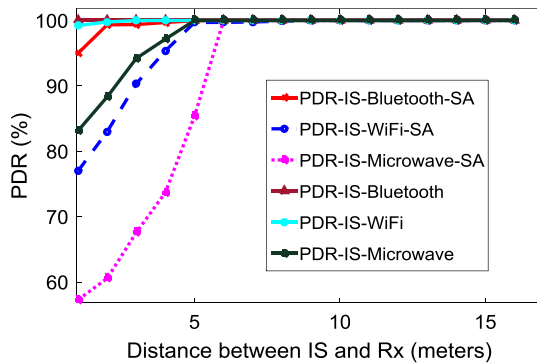


Fig. 32. PDR as a function of distance between Tx and Rx, $S_{IS-Rx} = 1\text{--}16\text{ m}$.

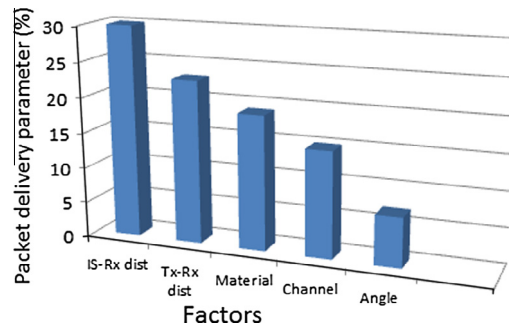


Fig. 34. Difference in average packet delivery parameter between the highest and lowest levels for each factor.



Fig. 35. Offset frequency measurement by RF spectrometer.

6. Conclusions and future work

Our approach is to coexist with these 2.4-GHz technologies, tolerating these interferences and building material without causing the disproportionate degradation. Over and over again the product functions in a controlled lab environment but gets the performance degradation due to other 2.4-GHz technologies in the building environment. We cannot change the standard architecture and functioning principle of other technologies, and are not allowed to change building materials such as a door, walls, and other household stuff. Now the question is how designers can get the optimum performance under these hostile operating environments? A designer can control the deployment approach and implementation of ZigBee protocol. There are procedures to mitigate the losses. The present research work helps researchers to find the best deployment approach for optimum output in the real world condition.

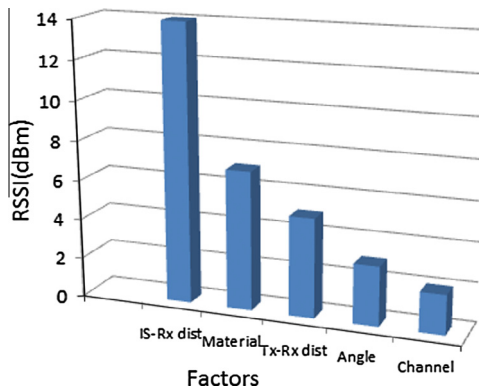


Fig. 33. Difference in average RSSI between the highest and lowest levels for each factor.

frequency, the SNR value of the Smart building was degrading. The frequency offset value, which we had noted for microwave oven, was ± 15 MHz, for WiFi ± 11 MHz and Bluetooth just ± 4 MHz. The whole setup for frequency offset measurement is shown in Fig. 35.

Every time for the particular deployment the designer has to perform the measurement and analysis as we have illustrated above.

References

- [1] Y. Lyu, F. Yan, Y. Chen, D. Wang, Y. Shi, N. Agoulmine, High-performance scheduling model for multisensor gateway of cloud sensor system-based smart-living, *Inf. Fusion* 21 (2015) 42–56.
- [2] G. Han, J. Jiang, L. Shu, J. Niu, H.-C. Chao, Management and applications of trust in wireless sensor networks: a survey, *Elsevier J. Comput. Syst. Sci.* 80 (3) (2014) 602–617.
- [3] <http://standards.ieee.org/about/get/802/802.15.html>.

- [4] S. Rodríguez, J.F. De Paz, G. Villarrubia, C. Zato, J. Bajo, J.M. Corchado, Multi-agent information fusion system to manage data from a WSN in a residential home, *Inf. Fusion* 23 (2015) 43–57.
- [5] M.L. Lee, A.K. Dey, Sensor-based observations of daily living for aging in place, *Pers. Ubiquit. Comput.* 19 (1) (2015) 27–43.
- [6] Y. Saleem, M.H. Rehmani, Primary radio user activity models for cognitive radio networks: a survey, *J. Netw. Comput. Appl.* 43 (2014) 1–16.
- [7] E. Kartsakli, A.S. Lalo, A. Antonopoulos, S. Tennina, M.D. Renzo, L. Alonso, C. Verikoukis, A survey on M2M systems for mHealth: a wireless communications perspective, *Sensors-Basel* 14 (10) (2014) 18009–18052.
- [8] S. Bhandari, S. Moh, A survey of MAC protocols for cognitive radio body area networks, *Sensors-Basel* 15 (4) (2015) 9189–9209.
- [9] P. Stenumgaard, J. Chilo, P. Ferrer-Coll, P. Angskog, Challenges and conditions for wireless machine-to-machine communications in industrial environments, *Commun. Mag., IEEE* 51 (6) (2013) 187–192.
- [10] A. Lazaro, D. Girbau, P. Moravek, R. Villarino, A study on localization in wireless sensor networks using frequency diversity for mitigating multipath effects, *Elektronika ir Elektrotechnika* 19 (3) (2013) 82–87.
- [11] S. Lim, S. Lee, J. Yoo, C.-K. Kim, NBP: light-weight Narrow Band Protection for ZigBee and Wi-Fi coexistence, *EURASIP J. Wirel. Commun. Netw.* 1 (2013) 1–13.
- [12] F. Sallabi, A. Gaouda, A. El-Hag, M. Salama, Evaluation of ZigBee wireless sensor networks under high power disturbances, *IEEE Trans. Power Deliv.* 29 (1) (2014) 13–20.
- [13] B. Zhen, H.-B. Li, S. Hara, R. Kohno, Clear channel assessment in integrated medical environments, *EURASIP J. Wirel. Commun. Netw.* (2008) 48.
- [14] L. Tytgat, O. Yaron, S. Pollin, I. Moerman, P. Demeester, Avoiding collisions between IEEE 802.11 and IEEE 802.15.4 through coexistence aware clear channel assessment, *EURASIP J. Wirel. Commun. Netw.* 2012 (1) (2012) 1–15.
- [15] A. Sikora, Compatibility of IEEE 802.15.4 (ZigBee) with IEEE 802.11 (WLAN), Bluetooth and Microwave Ovens in 2.4 GHz ISM-Band, Test Report, Steinbeis-Transfer Center, University of Cooperative Education, Lörrach, 2004.
- [16] A. Sikora, V.F. Groza, Coexistence of IEEE802. 15.4 with other Systems in the 2.4 GHz-ISM-Band', in: Proceedings of the IEEE Instrumentation and Measurement Technology Conference, IMTC, 16–19 May, Ottawa, 2005, pp. 1786–1791.
- [17] M. Petrova, J. Riihijarvi, P. Mahonen, S. Labella, Performance study of IEEE 802.15.4 using measurements and simulations, in: Wireless Communications and Networking Conference, WCNC 2006, 3–6 April, IEEE, Las Vegas, 2006, pp. 487–492.
- [18] P.L. Iturri, J.A. Nazábal, L. Azpilicueta, P. Rodriguez, M. Beruete, C. Fernández-Valdivielso, F. Falcone, Impact of high power interference sources in planning and deployment of wireless sensor networks and devices in the 2.4 GHz frequency band in heterogeneous environments, *Sensors* 12 (11) (2012) 15689–15708.
- [19] W. Guo, W.M. Healy, M. Zhou, Impacts of 2.4-GHz ISM band interference on IEEE 802.15.4 wireless sensor network reliability in buildings, *IEEE Trans. Instrum. Meas.* 61 (9) (2012) 2533–2544.
- [20] S. Lee, H. Shin, R. Ha, H. Cha, IEEE 802.15.4a CSS-based mobile object locating system using sequential Monte Carlo method, *Comput. Commun.* 38 (2014) 13–25.
- [21] <<https://www.qualcomm.com/invention/technologies/1000x/spectrum>> (accessed on 5 June 2015).
- [22] F. Cuomo, A. Abbagnale, E. Cipollone, Cross-layer network formation for energy-efficient IEEE 802.15.4/ZigBee wireless sensor networks, *Ad Hoc Netw.* 11 (2) (2013) 672–686.
- [23] M. Chen, J. Wan, S. González, X. Liao, V.C. Leung, A survey of recent developments in home M2M networks, *Commun. Surv. Tutor., IEEE* 16 (1) (2014) 98–114.
- [24] G. Li, P. Fan, K.B. Letaief, Rayleigh fading networks: a cross-layer way, *IEEE Trans. Commun.* 57 (2) (2009) 520–529.
- [25] I.F. Akyildiz, W. Su, Y. Sankarasubramaniam, E. Cayirci, A survey on sensor networks, *IEEE Commun. Mag.* 40 (8) (2002) 102–114.
- [26] R.-B. Zhang, J.-G. Guo, F.-H. Chu, Y.-C. Zhang, Environmental-adaptive indoor radio path loss model for wireless sensor networks localization, *AEU – Int. J. Electron. Commun.* 65 (12) (2011) 1023–1031.
- [27] P. Kulakowski, J. Vales-Alonso, E. Egea-López, W. Ludwin, J. García-Haro, Angle-of-arrival localization based on antenna arrays for wireless sensor networks, *Comput. Electr. Eng.* 36 (6) (2010) 1181–1186.
- [28] W.-S. Jang, W. Healy, Wireless sensor network performance metrics for building applications, *Energy Build.* 42 (6) (2010) 862–868.
- [29] K. Malhi, S.C. Mukhopadhyay, J. Schnepper, M. Haefke, H. Ewald, A Zigbee-based wearable physiological parameters monitoring system, *IEEE Sens. J.* 12 (3) (2012) 423–430.
- [30] N.K. Suryadevara, S.C. Mukhopadhyay, Wireless sensor network based home monitoring system for wellness determination of elderly, *IEEE Sens. J.* 12 (6) (2012) 1965–1972.
- [31] S.D.T. Kelly, N. Suryadevara, S.C. Mukhopadhyay, Towards the implementation of IoT for environmental condition monitoring in homes, *IEEE Sens. J.* 13 (10) (2013) 3846–3853.
- [32] H. Ghayvat, A. Nag, N. Suryadevara, S. Mukhopadhyay, X. Gui, J. Liu, Sharing research experiences of WSN based smart home, *Int. J. Smart Sens. Intell. Syst.* 7 (4) (2014) 1997–2013.
- [33] H. Ghayvat, S.C. Mukhopadhyay, X. Gui, Sensing Technologies for Intelligent Environments: A Review: Intelligent Environmental Sensing, Springer, 2015, pp. 1–31. ISBN 978-3-319-12891-7.
- [34] S. Mukhopadhyay, Wearable sensors for human activity monitoring: a review, *IEEE Sens. J.* 15 (3) (2015) 1321–1330.
- [35] H. Ghayvat, S. Mukhopadhyay, X. Gui, N. Suryadevara, WSN and IOT-based smart homes and their extension to smart buildings, *Sensors-Basel* 15 (5) (2015) 10350–10379.
- [36] Dual band versatility, <http://files.metageek.net/marketing/Wi-Spy_DBx/Wi-spy_DBx_medium.pdf> (accessed on 17 Jan 2015).
- [37] Powerful RF analyzer for Wi-Fi, <http://www.streakwave.com/metageek/Chan_Pro_medium.pdf> (accessed on 17 Jan 2015).